

New Limits on Interactions between Weakly Interacting Massive Particles and Nucleons Obtained with CsI(Tl) Crystal Detectors

S.C. Kim,¹ H. Bhang,¹ J.H. Choi,¹ W.G. Kang,² B.H. Kim,¹ H.J. Kim,³ K.W. Kim,¹
S.K. Kim,^{1,*} Y.D. Kim,² J. Lee,¹ J.H. Lee,¹ J.K. Lee,¹ M.J. Lee,¹ S.J. Lee,¹ J. Li,¹ J. Li,⁴
X.R. Li,¹ Y.J. Li,⁴ S.S. Myung,¹ S.L. Olsen,¹ S. Ryu,¹ I.S. Seong,¹ J.H. So,³ and Q. Yue⁴
(KIMS Collaboration)

¹*Department of Physics and Astronomy, Seoul National University, Seoul, 151-747, Korea*

²*Department of Physics, Sejong University, Seoul, 143-747, Korea*

³*Department of Physics, Kyungpook National University, Daegu, 702-701, Korea*

⁴*Department of Engineering Physics, Tsinghua University, Beijing, 100084, China*

(Dated: August 15, 2018)

New limits are presented on the cross section for Weakly Interacting Massive Particle (WIMP) nucleon scattering in the KIMS CsI(Tl) detector array at the Yangyang Underground Laboratory. The exposure used for these results is 24524.3 kg-days. Nuclei recoiling from WIMP interactions are identified by a pulse shape discrimination method. A low energy background due to alpha emitters on the crystal surfaces is identified and taken into account in the analysis. The detected numbers of nuclear recoils are consistent with zero and 90% confidence level upper limits on the WIMP interaction rates are set for electron equivalent energies from 3 keV to 11 keV. The 90% upper limit of NR event rate for 3.6-5.8 keV corresponding to 2-4 keV in NaI(Tl) is 0.0098 counts/kg/keV/day which is below the annual modulation amplitude reported by DAMA. This is incompatible with interpretations that enhance the modulation amplitude such as inelastic dark matter models. We establish the most stringent cross section limits on spin-dependent WIMP-proton elastic scattering for the WIMP masses greater than 20 GeV/ c^2 .

PACS numbers: 95.35.+2, 14.80.Ly

Astronomical observations have led to the conclusion that the majority of the matter in our universe is invisible, exotic and non-relativistic dark matter [1]. However, the identity of the dark matter is still not known. One possible source are WIMPs, which are candidates for particle dark matter that naturally occur in theories that extend the standard model of the particle physics for reasons independent of the dark matter problem [2]. There have been a number of experiments that search for WIMPs in our galaxy by looking for nuclei recoiling from WIMP-nucleus scattering [3, 4, 7, 9–16]. To date, there are several experiments that interpret their results as being possibly due to WIMP signals including DAMA, CoGeNT and CRESST [4–6]. In particular, the DAMA results have attracted considerable attention since it has reported observations of an annual modulation of WIMP-like signals with a claimed significance of 9σ [4]. This has spurred a continuing debate concerning the observation of WIMPs that has lasted for over a decade. WIMP-nucleon cross sections inferred from the DAMA modulation are in conflict with limits from other experiments that directly measure nuclear recoils [7, 9–17]. In attempts to reconcile these results, various schemes have been suggested, including the inelastic dark matter (iDM) model [19], in which an excited state of the dark matter particle is hypothesized and the dominant WIMP-nucleon scattering process involves a transition to this excited state. Recently, strong constraints on the allowed iDM model parameter space

have been reported [14, 18, 20, 21].

The KIMS (Korea Invisible Matter Search) collaboration is performing direct searches for WIMPs using CsI(Tl) detectors in the Yangyang Underground Laboratory (Y2L). CsI(Tl) is a commonly used scintillating crystal with ¹³³Cs and ¹²⁷I target elements that are sensitive to both spin-independent (SI) and spin-dependent (SD) interactions [3]. Furthermore, a pulse shape discrimination (PSD) technique makes it possible to distinguish nuclear recoil (NR)-induced signals from electron recoil (ER)-induced signals on a statistical basis. Results from the KIMS experiment based on a four-crystal array are reported in Ref. [7]. The detector has been upgraded to a 3×4 CsI(Tl) crystal array with total mass 103.4 kg. Each detection module consists of a low-background CsI(Tl) crystal ($8 \times 8 \times 30$ cm³) [8] with photomultiplier tubes (PMTs) mounted at each end. The data were collected between September 2009 and August 2010. The crystal array is surrounded by a shield consisting of: 10 cm of copper; 5 cm of polyethylene; 15 cm of lead; and 30 cm of liquid-scintillator-loaded mineral oil to stop external neutrons and gammas and veto cosmic-ray muons. The trigger condition is two or more photoelectrons (PEs) in each PMT within a 2 μ s time window. Amplified PMT signals are digitized by 400 MHz flash analog-to-digital converters (FADC); the total recorded time window for an event is 40 μ s, of which 25 μ s is analyzed. Since high energy muon interactions in the CsI(Tl) crystal can produce a long tail that may

last for several tens of milliseconds, we veto events that occur less than 50 milliseconds after a muon coincidence with the CsI(Tl) detector in the off-line analysis. The muon coincidence rate is 6-7 per hour and the dead time from this veto is negligible. In the energy region below 10 keV, PMT noise produces a serious background. To characterize PMT noise-induced events, a PMT Dummy Detector (PDD) module that has the same structure as a CsI(Tl) detector module with the crystal replaced by a clean, transparent and empty acrylic box is included in the shielded volume and operated simultaneously with the CsI(Tl) detector array. The event selection efficiency is detector-module dependent and ranges from 20~40% at 3 keV to 40~70% at 10 keV. Events that trigger two or more detector modules in the array are rejected off-line since a WIMP interacts only with the one nuclei in a detector: a NR event that is confined to a single detector module is the experimental signature for a WIMP-nucleus scattering.

We determine the NR event rate from a PSD analysis. To characterize the PSD, we use the quantity we call LMT10, which is the logarithm of the mean time of an event calculated over a 10 μ s interval that starts with the first detected PE. Specifically, MT10 (mean time over a 10 μ s) = $\frac{\sum_{t_i < 10 \mu s} A_i \times t_i}{\sum_{t_i < 10 \mu s} A_i}$, where A_i is the area of the i^{th} cluster, which is usually equivalent to a single PE, of an event.

We determine the expected LMT10 distribution for ER events by irradiating small CsI(Tl) crystals ($3 \times 3 \times 1.4$ cm³, test crystals 1 & 2) with gamma rays from a ¹³⁷Cs radioactive source and also from Compton scattering events detected in the array. The test crystals are small pieces that have been cut from the same ingots from which crystals used in WIMP search were also cut. The expected distributions for NR events were determined by exposing test crystal 2 to neutrons from a Am-Be source. With the higher sensitivity of the current exposure, we detected a previously unseen third component with a mean time distribution that is faster than that for NR events. Studies show that this originates from alpha decays of radioactive isotopes that adhere to the crystal surfaces, *i.e.*, surface alphas (SA), with characteristics described in detail in Ref. [23]. To determine the LMT10 distribution for SA events, we contaminated test crystal 1 with Rn progenies, and studied its response for events tagged as outgoing alphas from the crystal surface [23]. Figure 1 shows a comparison of the three different reference LMT10 distributions.

The test-crystal measurements were done at temperatures of $(25.4 \pm 0.3)^\circ\text{C}$ for SA and $(25.3 \pm 0.7)^\circ\text{C}$ for NR. Throughout the WIMP search data-taking period, the crystals were kept in the 20 ~ 21.6 $^\circ\text{C}$ temperature range, with variations that depend on the detector position; each detector had rms temperature fluctuations of $\sim 0.2^\circ\text{C}$. The mean values of the ER LMT10 dis-

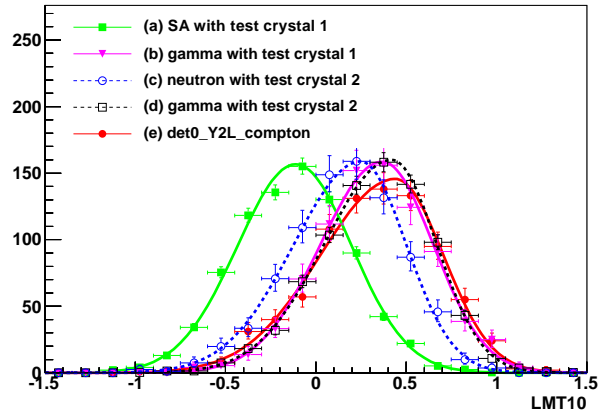


FIG. 1: LMT10 distributions at 3 keV for (a) SA with test crystal 1, (b) gammas with test crystal 1, (c) neutrons with test crystal 2, (d) gammas with test crystal 2 (e) Compton scattering events in detector 0 used in the WIMP search. This data sample is obtained at $(25.2 \pm 0.2)^\circ\text{C}$ for comparisons with other reference data.

tributions of the 12 detectors determined *in situ* have an average value of 0.62 with an *rms* spread of 0.035 for 59.54 keV gammas from an ²⁴¹Am source. Since the temperature conditions of the reference samples used to determine the NR and SA distributions are different, some adjustment is necessary. Previous studies [24, 25] have shown that the ratio $R_r = \tau_n/\tau_e$ is independent of temperature, where τ_n is the mean time of NR and τ_e , the mean time of ER. By comparing the LMT10 distribution from gamma irradiation on a test crystal and that of the crystals used in the WIMP search, we adjust the LMT10 distribution of NR events and SA events. We assume that there are only three components—NR, ER, and SA—in the WIMP search data and form the logarithm of the likelihood function for each energy bin as:

$$\begin{aligned}
 F_i &= -\log(\mathcal{L}) \\
 &= -\sum_{k=1}^{n_i} \log(f_{N,i}P_{N,i}(x_k) + f_{S,i}P_{S,i}(x_k) \\
 &\quad + (1 - f_{N,i} - f_{S,i})P_{E,i}(x_k)),
 \end{aligned}$$

where x_k is the LMT10 of the k^{th} event, the index i denotes the i^{th} energy bin, n_i is the number of events in the i^{th} energy bin, $P_{N,i}$, $P_{E,i}$ and $P_{S,i}$ are the probability density functions (PDFs) for NR, ER and SA, respectively, and $f_{N,i}$ and $f_{S,i}$ are the NR and SA event fractions in the i^{th} energy bin, respectively.

We determine $f_{N,i}$ and $f_{S,i}$ using the Bayesian Analysis Tool (BAT) program [26] with prior PDFs for $f_{N,i}$ and $f_{S,i}$ that are flat between 0 and 1. The Bayesian analysis produces posterior PDFs that reflect the degree of preference for the parameter values based on the experimental data. As an example, Fig. 2(a) shows contours of the two-dimensional posterior PDFs for $f_{N,i}$ and $f_{S,i}$ for the 6 keV energy bin in one of the detector modules.

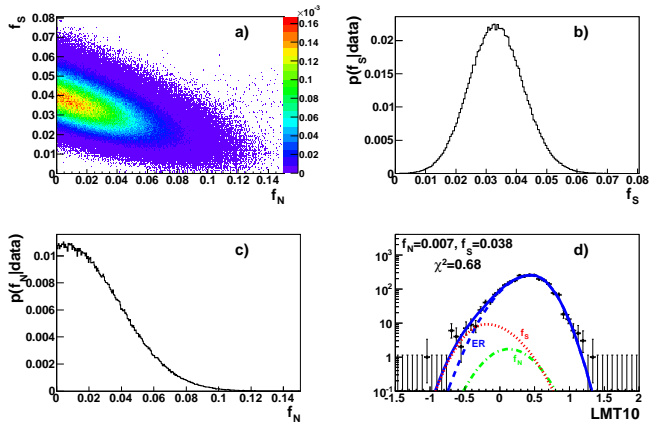


FIG. 2: **a)** Two-dimensional plot of $f_{N,i}$ (horizontal) versus $f_{S,i}$ (vertical). **b)** Projections of $f_{S,i}$ and **c)** $f_{N,i}$ for the 6 keV bin of detector 9. **d)** The fitted LMT10 distribution for the 6 keV bin of detector 9.

The posterior PDF of each parameter is the projection of the two-dimensional PDF onto that parameter's axis as shown in Figs. 2(b) and (c). To test the sensitivity to the choice of priors, we repeated this analysis with the flat prior PDF replaced with a Jeffrey's prior [27]. The Jeffrey's prior results agree with those with the flat prior within $1 \sim 2$ percent.

The NR event rate for each detector, determined from $f_{N,i}$ and the event selection efficiency, is shown in Fig. 3. The black horizontal bars indicate the 90% confidence level (C.L.) upper limits and the red vertical lines denote the 68% C.L. intervals. The red horizontal lines mark the most probable NR rate values.

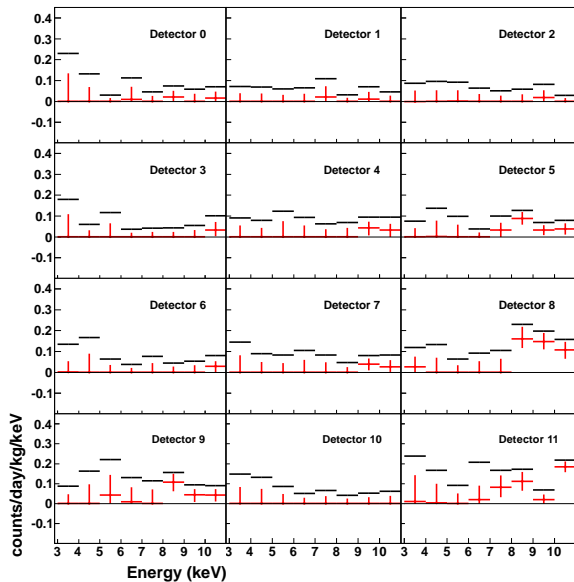


FIG. 3: Nuclear recoil event rates for all detectors. The black horizontal bar indicate 90% C.L. upper limits, the red vertical lines denote the 68% C.L. interval, and the red horizontal bars the most probable values.

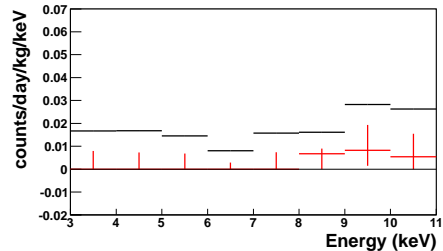


FIG. 4: Total nuclear recoil event rates from the combined results from nine detectors (without detector 0, 8 and 11).

The rates of SA events in the 3-11 keV energy range averaged over the detector modules are shown in Table I. The SA background levels of detectors 0, 8 and 11 are about three times as high as the average of the remaining detectors. For this reason, these three detectors are excluded from the average NR event rate determination. This reduces the total exposure used in the final analysis to 24524.3 kg-days. Figure 4 shows the 68% C.L. intervals and 90% C.L. upper limits on the NR event rate from the combined PDF of the remaining nine detector modules. These limits include systematic effects from uncertainties in the LMT10 PDFs for each event type and their crystal-to-crystal deviations. No significant excess of NR events is observed.

Assuming the standard halo model [28], we translate these measurements to the cross section limits for WIMP-nucleon SI interactions and WIMP-proton SD interactions that are presented in the left and right panels of Fig. 5, respectively. The limits shown in the two figures are about one order-of-magnitude more stringent than the previous KIMS results [7], due primarily to the identification of the SA background component and the larger exposure. The WIMP-proton SD interaction cross section limits are the most stringent to date.

The NR event rate limits also have important implications for the interpretation of the DAMA annual modulation signal, which has an amplitude of 0.0183 ± 0.0022 counts/day/kg/keV in the 2-4 keV energy range in NaI(Tl) scintillators [4]. Considering the different quenching factors of Iodine for NaI(Tl) and CsI(Tl) [3, 29], the 2-4 keV DAMA energy range corresponds to 3.6-5.8 keV in KIMS, which is included in the first

SA contamination level (counts/day/kg/keV)			
Detector	Level	Detector	Level
0	0.203 ± 0.026	6	0.087 ± 0.021
1	0.071 ± 0.017	7	0.076 ± 0.025
2	0.066 ± 0.020	8	0.238 ± 0.025
3	0.089 ± 0.024	9	0.123 ± 0.025
4	0.039 ± 0.020	10	0.014 ± 0.026
5	0.064 ± 0.018	11	0.205 ± 0.024

TABLE I: SA contamination level for each detector averaged over the 3-10 keV energy bins.

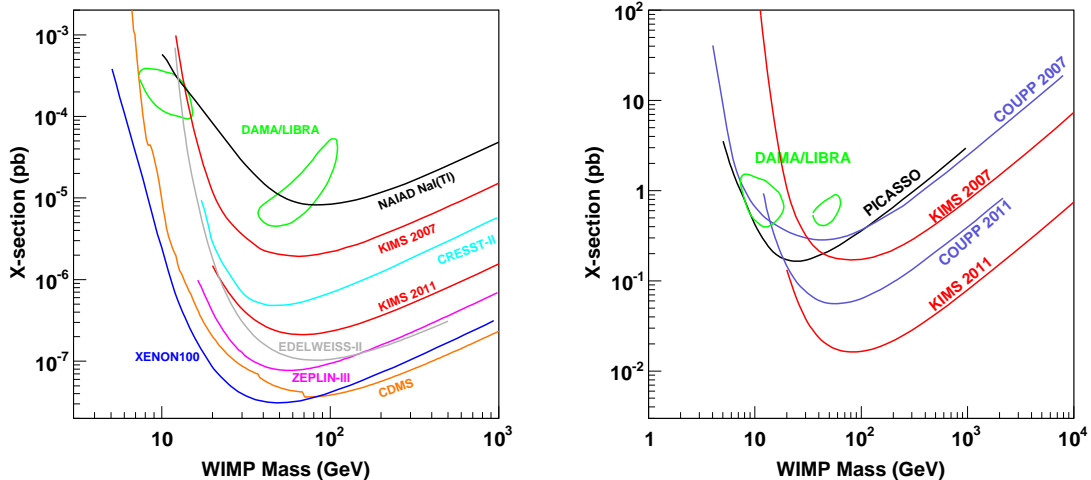


FIG. 5: The 90 % exclusion limits on **(Left)** SI WIMP-nucleon and **(Right)** SD WIMP-proton cross sections. In both plots DAMA results interpreted by Savage *et al.* [17] are used (3σ contours are drawn). The SI plot includes NAIAD [9], CRESST-II [10], EDELWEISS-II [11], ZEPLIN-III [12], XENON100 [13] and CDMS [14] limits. The SD plot includes PICASSO [15] and COUPP [16] limits.

three bins in Fig. 4. Our 90% C.L. upper limit on the NR event rate in the 3.6-5.8 keV energy range is 0.0098 counts/day/kg/keV, which is well below the DAMA signal amplitude. Therefore, any scenario involving Iodine as the target, such as the iDM model, is incompatible with our limits. As an example, the parameter space allowed for DAMA in the iDM model and our exclusion limits for a WIMP of mass 70 GeV are presented in Fig. 6. An alternative iDM interpretation considers Thallium, which is present at the 10^{-3} level in both the DAMA and KIMS detectors [22], as the dominant target, can be addressed by our results. We estimate the quenching factors for Thallium in NaI(Tl) and CsI(Tl) using a semi-empirical calculation [30] and find $\frac{Q_{\text{CsI}}^{\text{I,Tl}}}{Q_{\text{NaI}}^{\text{I,Tl}}} \approx \frac{Q_{\text{CsI}}^{\text{Tl}}}{Q_{\text{NaI}}^{\text{Tl}}}$, where $Q_{\text{CsI,NaI}}^{\text{I,Tl}}$ is the quenching factors of CsI(Tl) and NaI(Tl) for iodine and thallium ions. This indicates that the corresponding energy range in KIMS for Thallium is about the same as that for Iodine. Therefore our conclusion does not change when Thallium is considered as the dominant target.

In conclusion, we report improved limits for WIMP-nucleon cross sections using a data sample collected with a 103.4 kg CsI(Tl) scintillator detector array with a total exposure of 24524.3 kg-days. We identified and characterized a low energy background due to a contamination of alpha emitters on the surfaces of the crystals and incorporated it into the PSD analysis. No significant signals for NR events are observed and we determine 90% C.L. upper limits on NR event rates, and improved limits on WIMP-nucleon cross sections, including the most stringent limits to date on WIMP-proton SD scattering. The NR event rate upper limit is below the DAMA/LIBRA annual modulation amplitude in the corresponding en-

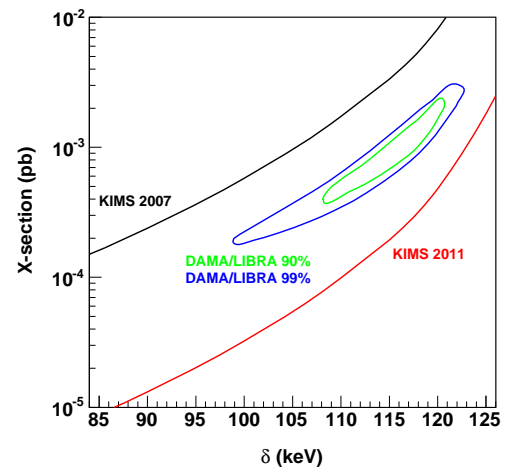


FIG. 6: The allowed parameter space for DAMA/LIBRA [19] and the limits reported here for a 70 GeV WIMP mass in iDM model. δ is the mass split between the ground and excited states of the WIMP. The astronomical parameters from Ref. [19] are used.

ergy region, disfavoring iDM model interpretations.

We are very grateful to the Korea Midland Power Co. and Korea Hydro and Nuclear Power Co. for providing the underground laboratory space at Yangyang. This research was supported by the WCU program (R32-10155) and Basic Science Research Grant (KRF-2007-313-C00155) through the National Research Foundation funded by the Ministry of Education, Science and Technology of Korea.

* skkim@hep1.snu.ac.kr

- [1] E. Komatsu *et al.*, ApJS **192**, 18 (2011).
- [2] G. Bertone, D. Hooper, and J. Silk, Phys. Rep. **405**, 279 (2005). L. Bergstrom, New J. Phys. **11**, 105006 (2009).
- [3] S. K. Kim *et al.*, New J. Phys. **12**, 075003 (2010).
- [4] R. Bernabei *et al.*, Eur. Phys. J. C **67**, 39 (2010).
- [5] C. E. Aalseth *et al.*, PRL **107**, 141301 (2011).
- [6] G. Angloher *et al.*, arXiv:astro-ph/1109.0702.
- [7] H. S. Lee *et al.*, Phys. Rev. Lett. **99**, 091301 (2007).
- [8] H. S. Lee *et al.*, Nucl. Instrum. Methods **571**, 644 (2007).
- [9] G. J. Alner *et al.*, Phys. Lett. B **616**, 17 (2005).
- [10] G. Angloher *et al.*, Astropart. Phys. **31**, 270 (2009).
- [11] E. Armengaud *et al.*, Phys. Lett. B **687**, 294 (2010).
- [12] V. N. Lebedenko *et al.*, Phys. Rev. D **80**, 052010 (2009).
- [13] E. Aprile *et al.*, Phys. Rev. Lett. **105**, 131302 (2010).
- [14] Z. Ahmed *et al.*, science **327**, 1619 (2010).
- [15] S. Archambault *et al.*, Phys. Lett. B **682**, 185 (2009).
- [16] E. Behnke *et al.*, Phys. Rev. Lett. **106**, 021303 (2011).
- [17] C. Savage *et al.*, JCAP **04**, 010 (2009).
- [18] K. Schmidt-Hoberg and M. W. Winkler, JCAP **09**, 010 (2009).
- [19] S. Chang *et al.*, Phys. Rev. D **79**, 043513 (2009).
- [20] D.Y. Akimov *et al.*, Phys. Lett. B **692**, 180 (2010).
- [21] E. Aprile *et al.*, arXiv:astro-ph/1104.3121.
- [22] S. Chang *et al.*, Phys. Rev. Lett. **106**, 011301 (2011).
- [23] S. C. Kim *et al.*, arXiv:1108.4353 (2011).
- [24] V. A. Kudryavtsev *et al.*, Astropart. Phys. **19**, 691 (2003).
- [25] H. S. Lee, Ph.D thesis, Seoul Nat. Univ. (2007).
- [26] A. Caldwell *et al.*, Comp. Phys. Comm **180**, 2197 (2009).
- [27] K. Nakamura *et al.* (Particle Data Group), J. Phys. G **37**, 075021 (2010).
- [28] J.D. Lewin and P.F. Smith, Astropart. Phys. **6**, 87 (1996).
- [29] H. S. Park *et al.*, Nucl. Instrum. Methods **491**, 460 (2002).
- [30] V. I. Tretyak, Astropart. Phys. **33**, 40 (2010).